Electronic Supporting Information

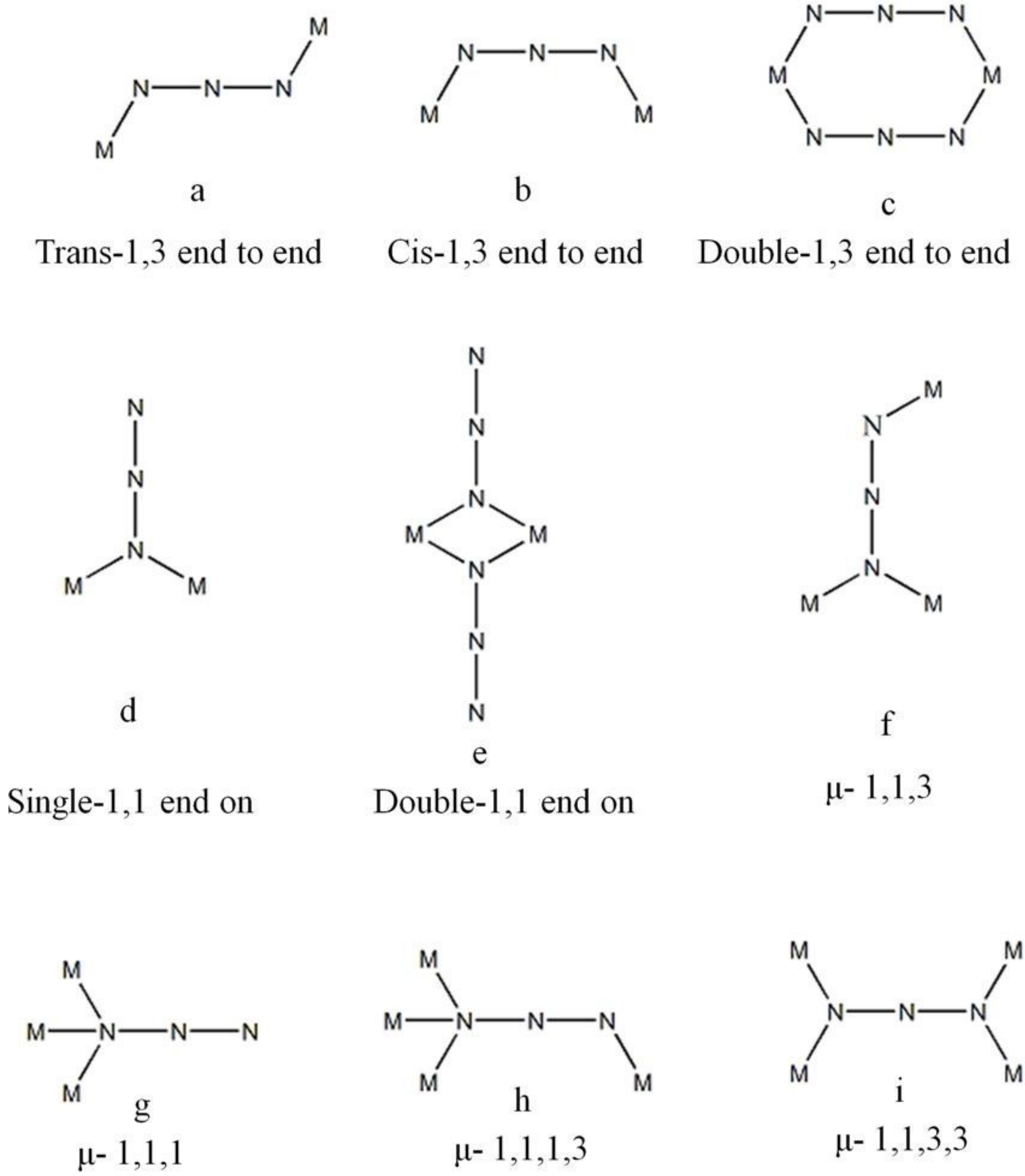
a
Trans-1,3 end to end
b
Cis-1,3 end to end
c
Double-1,3 end to end
d
Single-1,1 end on
e
Double-1,1 end on
f
μ- 1,1,3
g
μ- 1,1,1
h
μ- 1,1,1,3
i
μ- 1,1,3,3

Scheme 1

Table S1: Synthesis composition employed for the preparation of compounds **I- II.**

S no.	Composition (mM)	Product	Duration	Yield (%)
1.	0.5 mM $Cu(ClO_4)_2$ + 0.15mM 1,2-DAP + 0.15mM DETA + 1mM NaN_3	$[Cu_7(N_3)_{14}(C_3H_{10}N_2)(C_4H_{13}N_3)]_n$ (**I**)	14 days	82
2.	0.5 mM $Cu(ClO_4)_2$ + 0.15mM 1,2-DAP + 0.15mM N-2AE-1,3-PDA + 1mM NaN_3	$[Cu_7(N_3)_{14}(C_3H_{10}N_2)(C_5H_{15}N_3)_2]_n$ (**II**)	14 days	75

Yields are calculated based on the respective metals. Compositions given are the molar composition. CHN analysis for compound **I**: Calc(%) C 6.9; H 1.9; N 54.4; Found C 6.6; H 2.1; N 51.0 (%), CHN analysis for compound **II**: Calc(%) C 7.8; H 2.0; N 53.7; Found C 7.2; H 1.9; N 50.3 (%).

Table S2: calculated 'τ' and other parameters for compound **I –II:**

Compound **I**	τ values	% tetragonal elongation	% trigonal compression	Coordination geometry
Cu(2)	0.38	16.1	0.65	distorted *sp*
Cu(3)	0.22	29.3	-1.3	distorted *sp*
Cu(4)	0.27	24.0	0.3	distorted *sp*
Cu(6)	0.21	19.7	0.5	distorted *sp*
Compound **II**	τ values	% tetragonal elongation	% trigonal compression	Coordination geometry
Cu(2)	0.37	16.2	0.05	distorted *sp*
Cu(3)	0.21	30.8	0.96	distorted *sp*
Cu(4)	0.25	21.1	-0.40	distorted *sp*
Cu(6)	0.29	17.2	-1.1	distorted *sp*

Table S3: Selected observed bond distances in the compounds **I - II**.

Bond	Distance (Å)	Bond	Distance (Å)
Compound **I**			
Cu(1)-N(1)	1.997(6)	Cu(4)#1- N(27)	1.991(5)
Cu(1)-N(2)	2.005(6)	Cu(4)- N(36)	1.979(5)
Cu(1)-N(6)	2.039(5)	Cu(4)- N(39)	1.985(5)
Cu(1)-N(9)	2.032(5)	Cu(5)-N(18)	1.979(5)
Cu(1)-N(12)	2.510(2)	Cu(5)- N(21)	2.028(5)
Cu(2)-N(6)	1.979(5)	Cu(5)#2- N(30)	1.948(5)
Cu(2)-N(12)	1.997(5)	Cu(5)- N(33)	1.957(5)
Cu(2)-N(18)	2.017(5)	Cu(6)-N(33)	2.411(6)
Cu(2)- N(21)	2.008(5)	Cu(6)#1-N(36)	2.013(5)
Cu(2)- N(21)	2.008(5)	Cu(6)#1-N(39)	2.003(5)
Cu(2)-N(30)	2.320(5)	Cu(6)-N(42)	1.965(5)
Cu(3)-N(9)	1.984(5)	Cu(6)- N(45)	1.986(5)
Cu(3)-N(12)	2.584(1)	Cu(7)-N(3)	2.015(6)
Cu(3)-N(15)	1.961(5)	Cu(7)-N(4)	2.018(9)
Cu(3)- N(24)	1.974(5)	Cu(7)-N(5)	1.951(7)
Cu(3)- N(27)	1.998(5)	Cu(7)-N(14)	2.629(1)
Cu(4)-N(15)	2.460(6)	Cu(7)- N(42)	2.539(1)
Cu(4)#1- N(24)	1.962(5)	Cu(7)- N(45)	1.994(6)
Compound **II**			
Cu(1)-N(1)	2.001(7)	Cu(4)-N(36)	1.972(6)
Cu(1)-N(2)	1.980(7)	Cu(4)-N(39)	1.996(6)
Cu(1)-N(6)	2.025(6)	Cu(5)-N(18)	1.976(6)
Cu(1)-N(9)	2.025(6)	Cu(5)- N(21)	2.033(6)
Cu(1)-N(12)	2.533(7)	Cu(5)-N(30)	1.954(6)
Cu(2)-N(6)	1.987(6)	Cu(5)-N(33)	1.953(6)
Cu(2)-N(12)	1.989(6)	Cu(6)-N(33)	2.359(6)
Cu(2)- N(18)	2.012(6)	Cu(6)-N(36)	2.015(6)
Cu(2)- N(21)	2.016(6)	Cu(6)-N(39)	1.995(6)
Cu(2)#2-N(30)	2.339(6)	Cu(6)-N(42)	1.957(6)
Cu(3)-N(9)	1.971(6)	Cu(6)-N(45)	1.975(6)
Cu(3)-N(12)	2.589(2)	Cu(7)-N(3)	1.963(7)
Cu(3)-N(15)	1.955(6)	Cu(7)-N(4)	2.035(12)
Cu(3)-N(24)	1.981(6)	Cu(7)-N(5)	1.947(8)
Cu(3)-N(27)	1.996(6)	Cu(7)-N(14)	2.669(5)
Cu(4)#1- N(15)	2.417(6)	Cu(7)- N(42)	2.503(4)
Cu(4)- N(24)	1.959(6)	Cu(7)-N(45)	2.021(7)
Cu(4)-N(27)	1.988(6)		

Table S4: Cu(II)-$N_{EO(1,1)}$-Cu(II) bond angle table for compound **I –II:**

Angle	Amplitude(°)	Angle	Amplitude(°)
Compound **I**		Compound **II**	
Cu(1)-N(6)-Cu(2)	111.6(2)	Cu(1)-N(6)-Cu(2)	112.2(3)
Cu(3)-N(9)-Cu(1)	114.48(0)	Cu(3)-N(9)-Cu(1)	115.1(3)
Cu(1)-N(12)-Cu(2)	94.37(0)	Cu(1)-N(12)-Cu(2)	94.10(1)
Cu(3)-N(12)-Cu(1)	83.04(0)	Cu(3)-N(12)-Cu(1)	82.31(1)
Cu(3)-N(12)-Cu(2)	96.0(0)	Cu(3)-N(12)-Cu(2)	95.35(1)
Cu(3)-N(15)-Cu(4)	113.8(3)	Cu(3)-N(15)-Cu(4)#1	116.6(3)
Cu(5)-N(18)-Cu(2)	102.5(2)	Cu(5)-N(18)-Cu(2)	102.9(2)
Cu(2)-N(21)-Cu(5)	101.1(2)	Cu(2)-N(21)-Cu(5)	100.8(3)
Cu(4)#1-N(24)-Cu(3)	102.3(2)	Cu(4)-N(24)-Cu(3)	102.4(3)
Cu(4)#1-N(27)-Cu(3)	100.4(2)	Cu(4)-N(27)-Cu(3)	100.8(3)
Cu(5)#2-N(30)-Cu(2)	105.9(2)	Cu(5)-N(30)-Cu(2)#2	105.1(3)
Cu(5)-N(33)-Cu(6)	104.0(2)	Cu(5)-N(33)-Cu(6)	107.2(3)
Cu(4)-N(36)-Cu(6)#1	100.3(2)	Cu(4)-N(36)-Cu(6)	101.0(3)
Cu(4)-N(39)-Cu(6)#1	100.4(2)	Cu(4)-N(39)-Cu(6)	100.8(3)
Cu(6)-N(42)-Cu(7)	93.34(1)	Cu(6)-N(42)-Cu(7)	93.34(1)
Cu(6)-N(45)-Cu(7)	109.5(2)	Cu(6)-N(45)-Cu(7)	109.6(3)

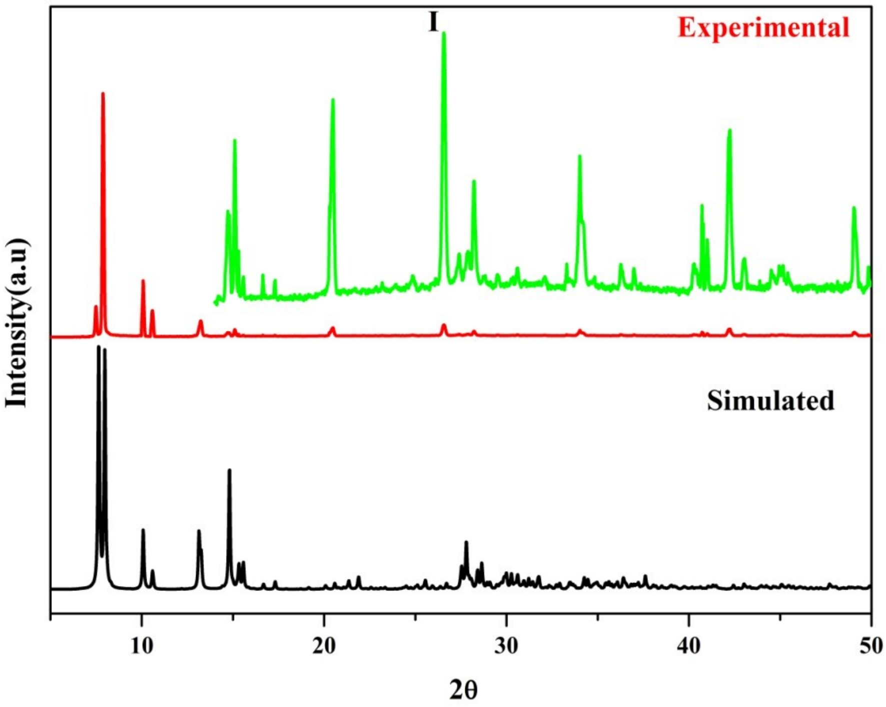

Fig. S1: Powder XRD (Cu kα) patterns of the compound **I**

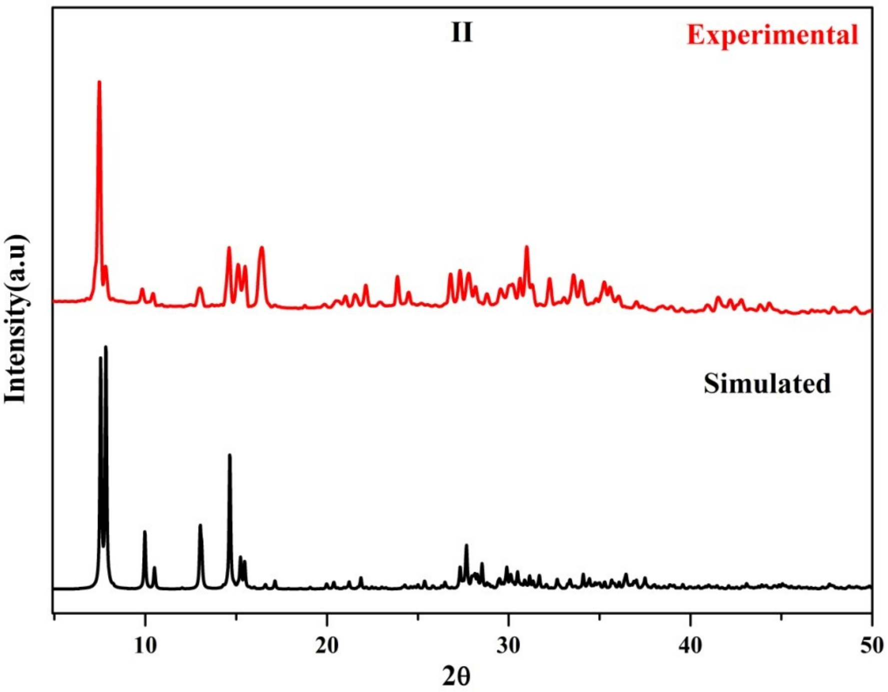

Fig. S2: Powder XRD (Cu kα) patterns of the compound **II**

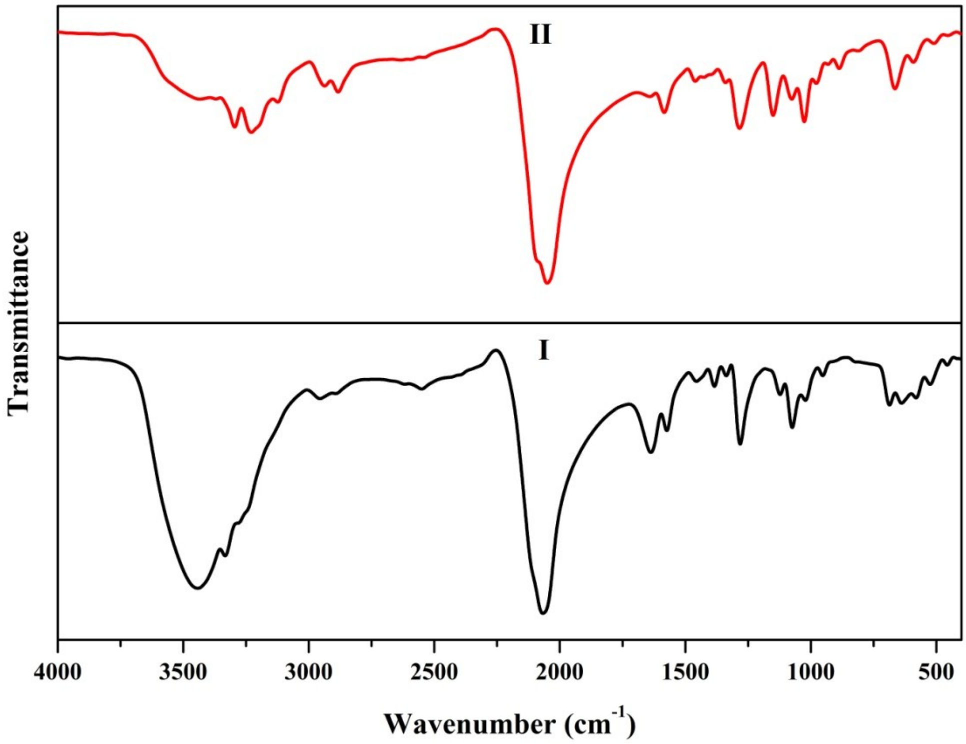

Fig. S3: IR spectra for the compounds **I-II**

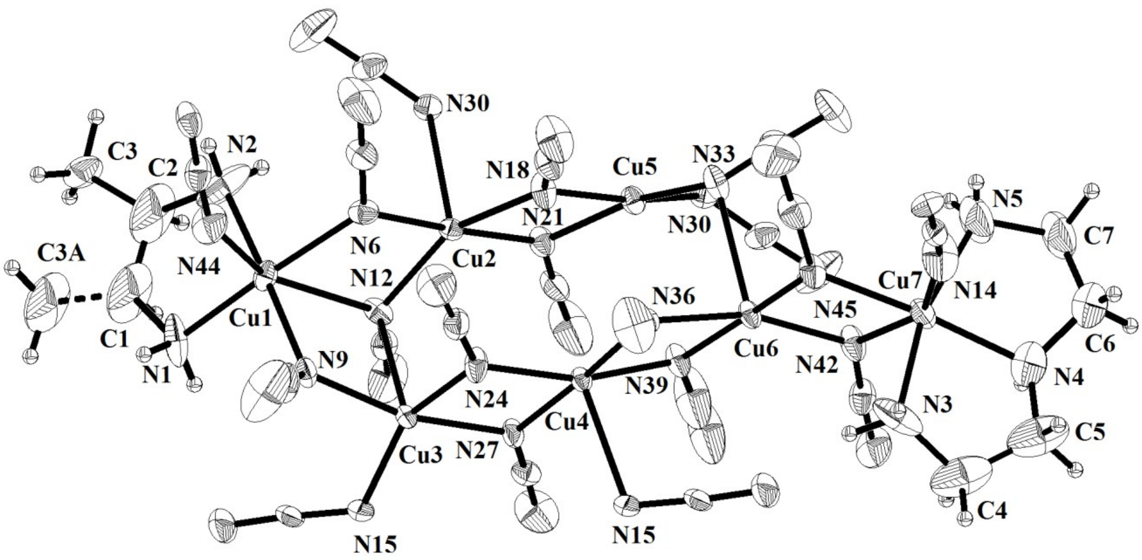

Fig. S4: Asymmetric unit in compound **I** (thermal ellipsoids with 50% probability)

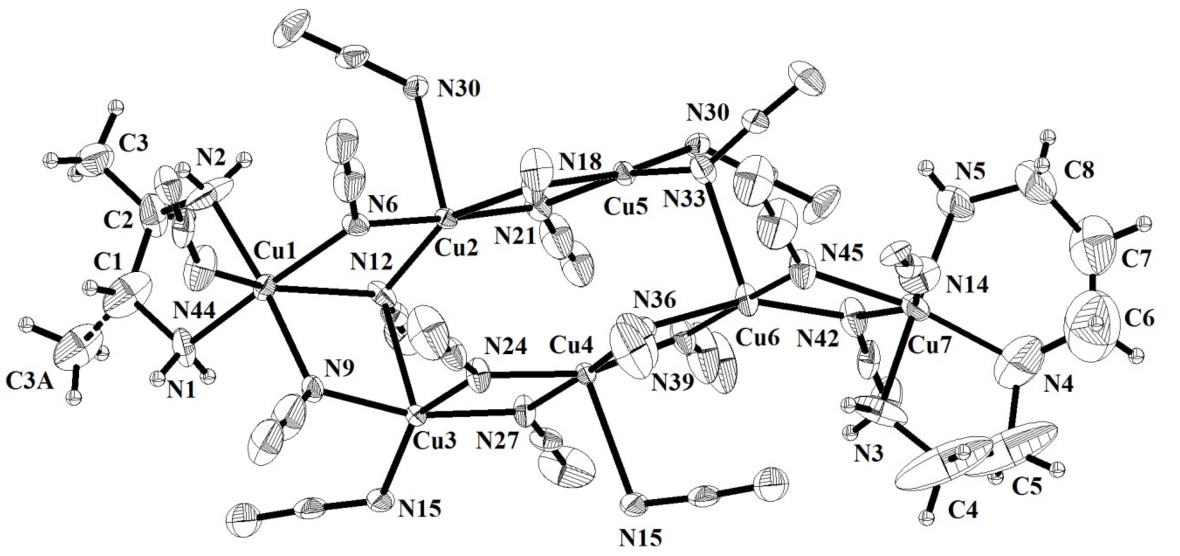

Fig. S5: Asymmetric unit in compound **II** (thermal ellipsoids with 50% probability)

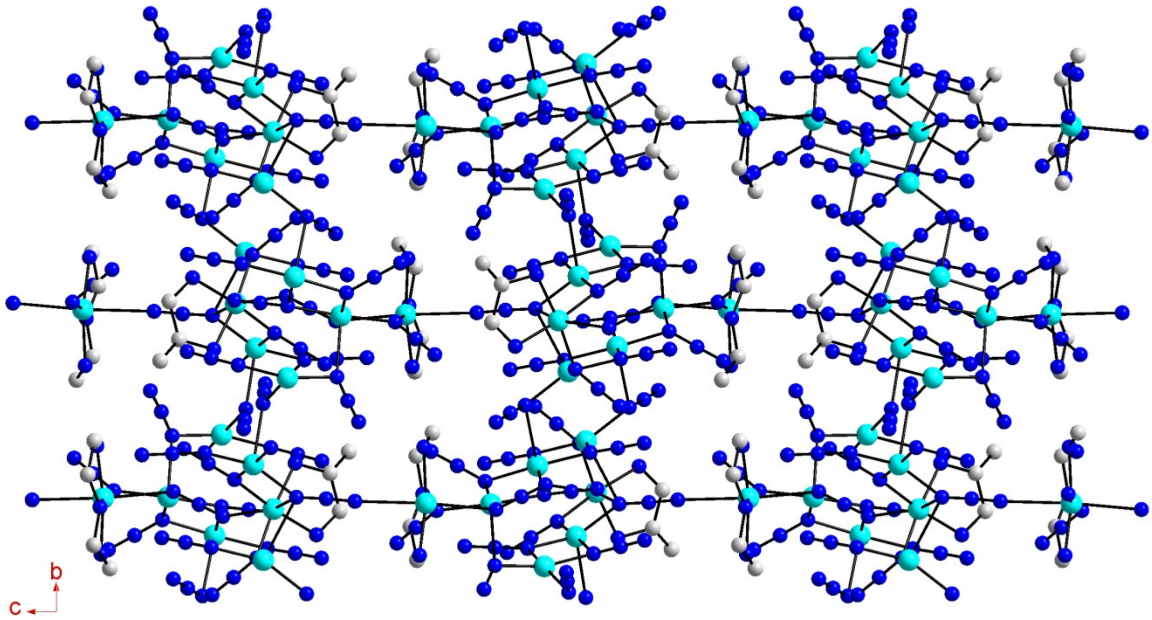

Fig. S6: 3D view of compound **I** from crystallographic axis **a.**

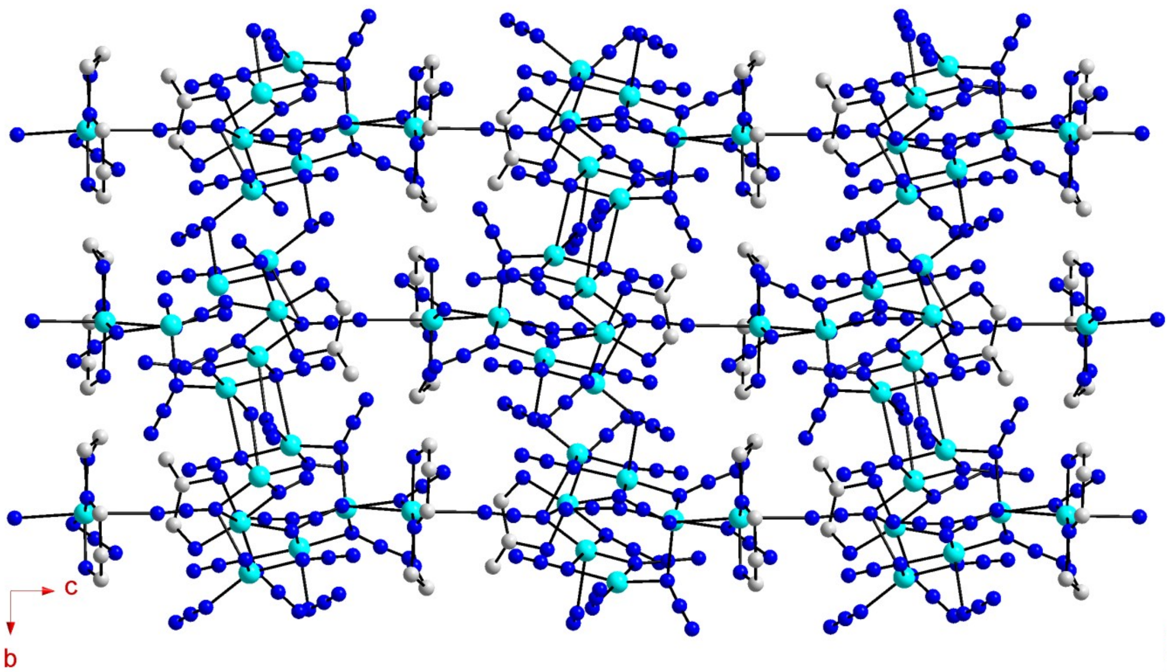

Fig. S7: 3D view of compound **II** from crystallographic axis a.

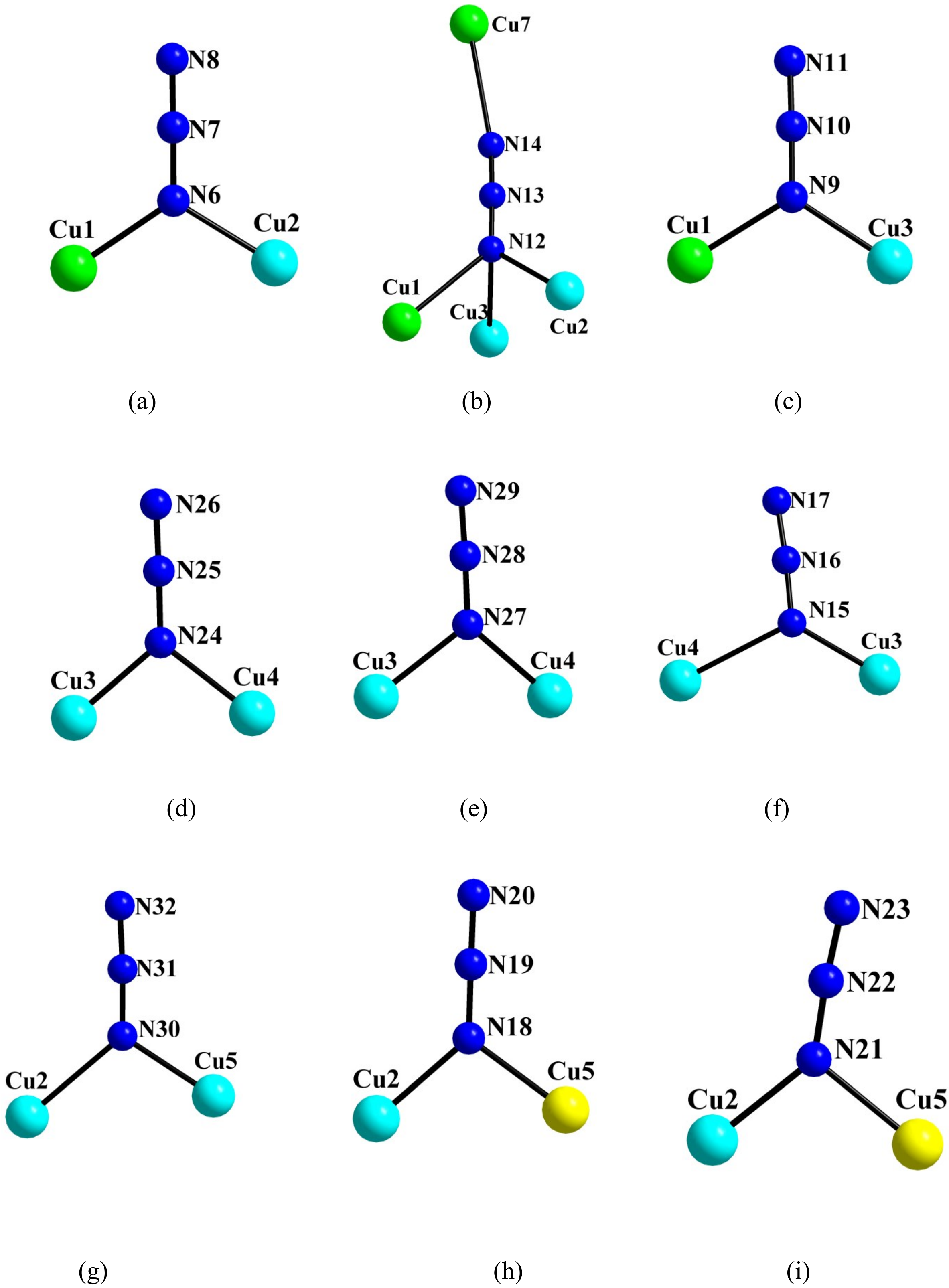
Cu7
N8
N7
N6
Cu1
Cu2
N14
N13
N12
Cu1
Cu3
Cu2
N11
N10
N9
Cu1
Cu3
(a)
(b)
(c)
N26
N25
N24
Cu3
Cu4
N29
N28
N27
Cu3
Cu4
N17
N16
N15
Cu4
Cu3
(d)
(e)
(f)
N32
N31
N30
Cu2
Cu5
N20
N19
N18
Cu2
Cu5
N23
N22
N21
Cu2
Cu5
(g)
(h)
(i)

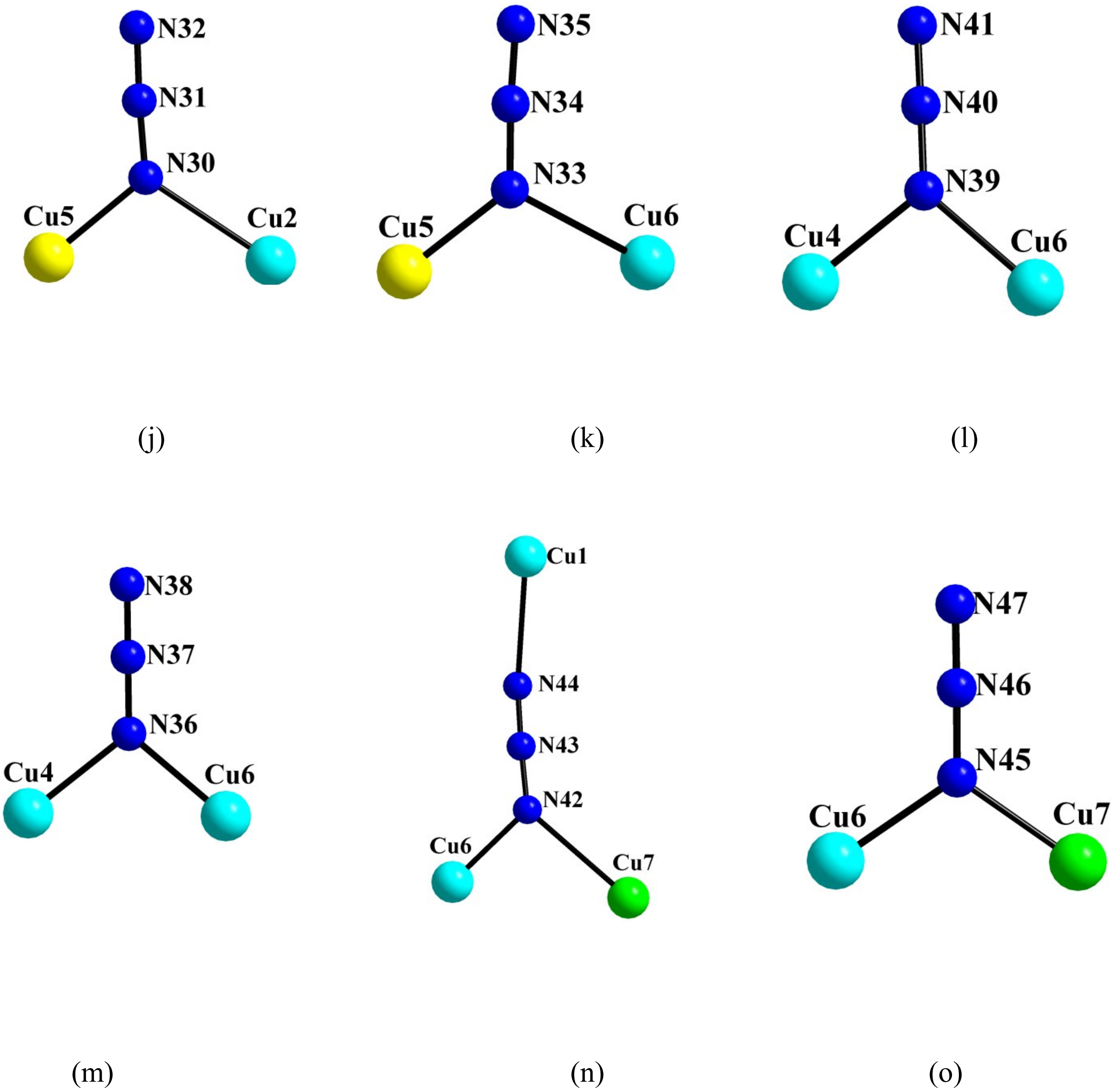

Fig. S8: View of various azide connectivity present in compound **I**.

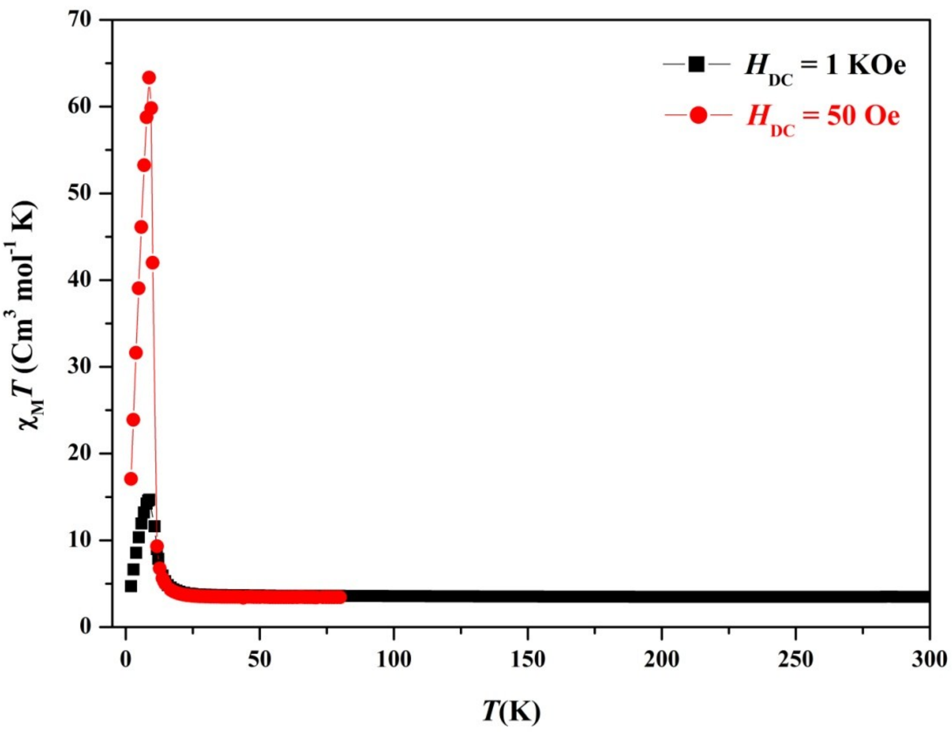

Fig. S9: Compound **I**: $\chi_M T = f(T)$ for H_{DC} = 1 kOe (in black) and 50 Oe (in red).

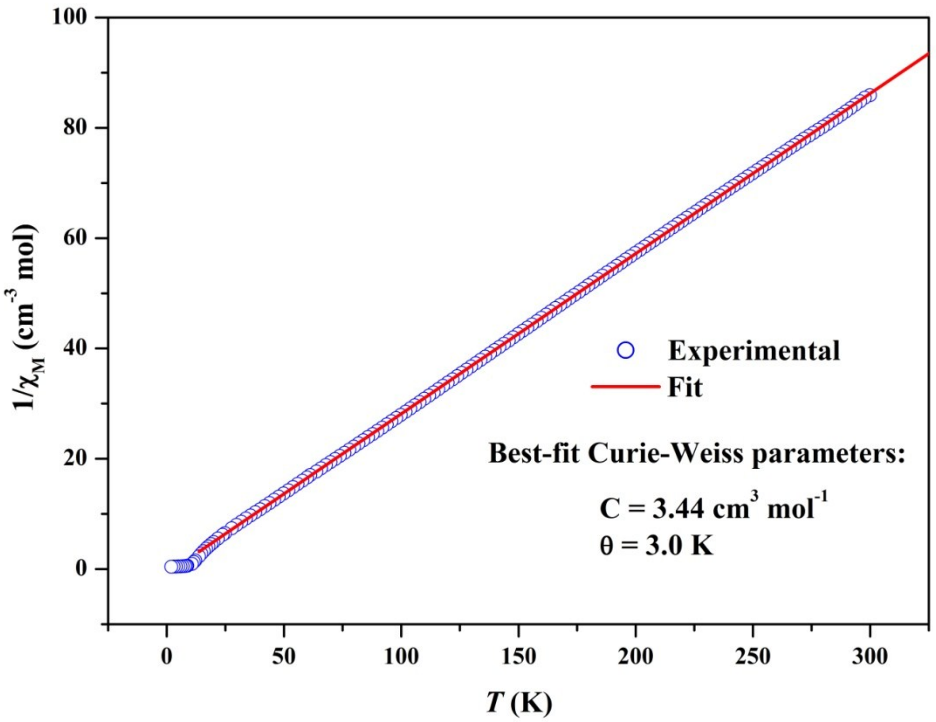

Fig. S10: $1/\chi_M = f(T)$ and Curie-Weiss best fit (considered T range, 300 – 40 K).

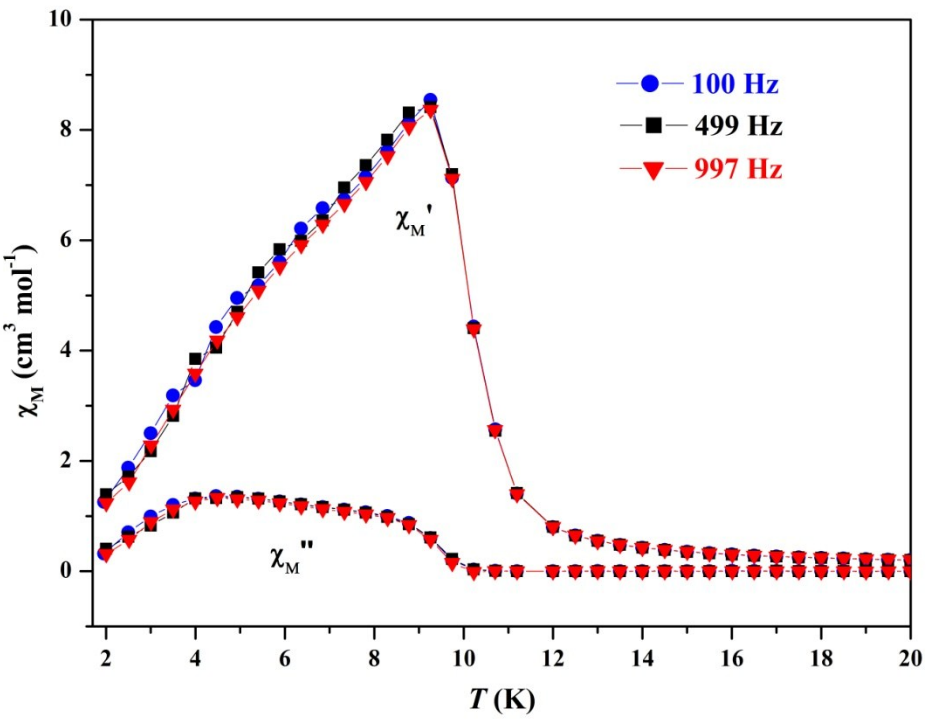

Fig. S11: The thermal variation of the in- (χ_M') and out-of-phase (χ_M'') magnetic susceptibility for **I** obtained for H_{AC} = 3 Oe and frequency of 100 Hz, 499 Hz, and 997 Hz.

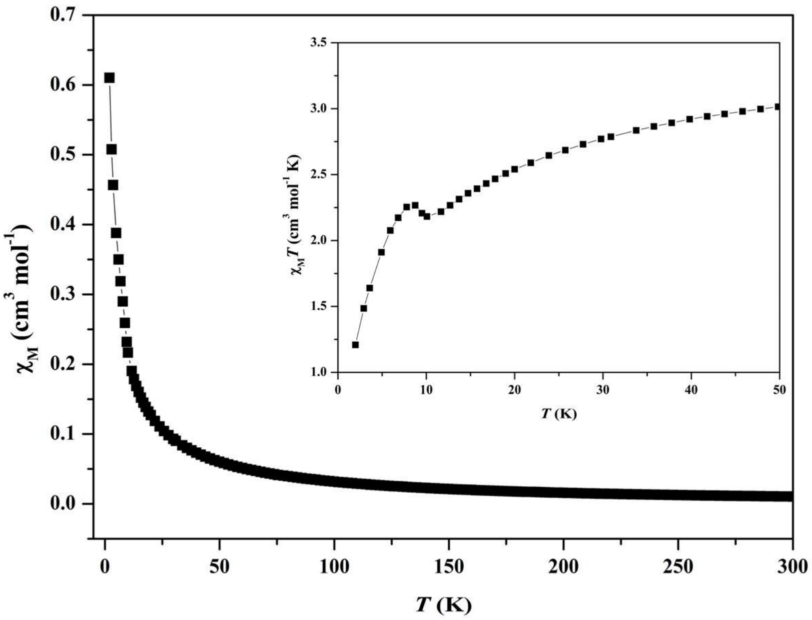

Fig. S12: The thermal variation of the magnetic susceptibility (χ_M) for compound **II,** (Inset) Variation of $\chi_M T$ as function of temperature (50 – 2 K).

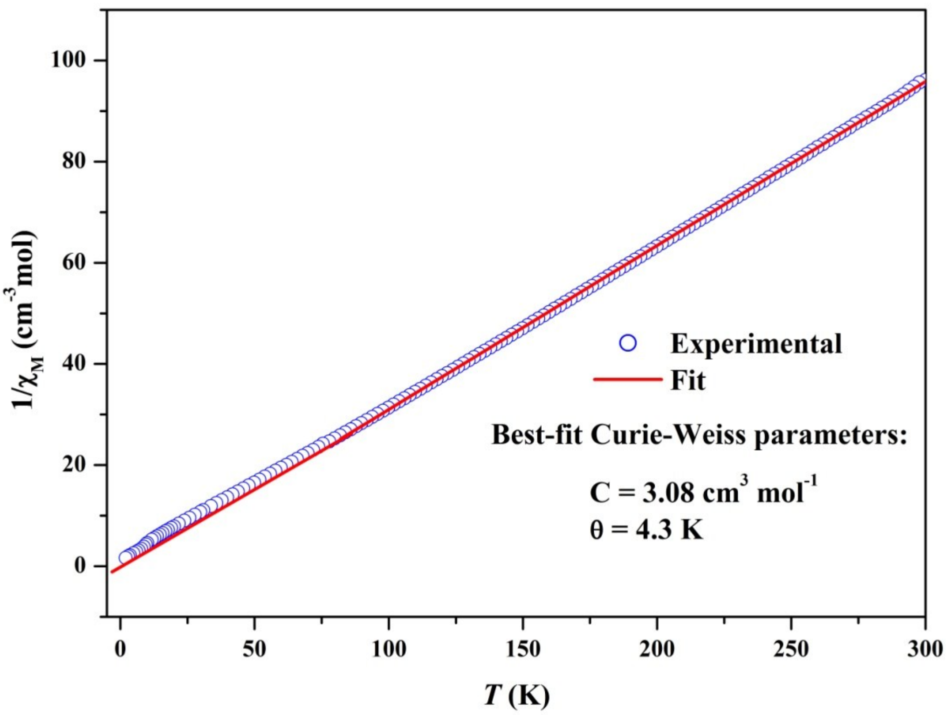

Fig. S13: $1/\chi_M = f(T)$ and Curie-Weiss best fit (considered *T* range, 300 – 100 K).